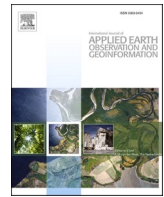




Contents lists available at ScienceDirect

# International Journal of Applied Earth Observations and Geoinformation

journal homepage: [www.elsevier.com/locate/jag](http://www.elsevier.com/locate/jag)



## Automated mapping of cultural heritage in Norway from airborne lidar data using faster R-CNN



Øivind Due Trier <sup>a,\*</sup>, Jarle Hamar Reksten <sup>a</sup>, Kristian Løseth <sup>b</sup>

<sup>a</sup> Norwegian Computing Center, Section for Earth Observation, Gaustadalléen 23A, P.O. Box 114 Blindern, NO-0314 Oslo, Norway

<sup>b</sup> The Directorate for Cultural Heritage in Norway, Dronningens Gate 13, P.O. Box 1483 Vika, NO-0116 Oslo, Norway

### ARTICLE INFO

#### Keywords:

Airborne laser scanning  
Deep learning  
Artificial intelligence  
Grave mounds  
Deer hunting systems  
Charcoal kilns

### ABSTRACT

The existing cultural heritage mapping in Norway is incomplete. Some selected areas are mapped well, while the majority of areas only contain chance discoveries, often with bad positional accuracy. The goal of this research was to develop automated tools for improving the cultural heritage mapping in Norway, thus enabling detailed mapping of large areas within realistic budgets and time frames. The focus was on three types of cultural heritage that occur frequently in many types of Norwegian landscape: grave mounds, pitfall traps in deer hunting systems and charcoal kilns.

A recent development in deep neural networks for object detection in natural images is the region-proposing convolutional neural network (R-CNN), which may also be used for cultural heritage detection in local relief model (LRM) visualizations of airborne laser scanning (ALS) data. Python code for 'Simple Faster R-CNN' was downloaded from Github.

On 737 test images ( $16.6 \text{ km}^2$ ) not seen during training, 87 % of the true cultural heritage objects were correctly identified, while 24 % of the predicted cultural heritage locations were false. However, all test images were small ( $150 \text{ m} \times 150 \text{ m}$ ) and contained at least one cultural heritage object, meaning that the false positive rate may be higher for an entire landscape. In Larvik municipality, Vestfold and Telemark County, on a  $67 \text{ km}^2$  area not seen during training, the R-CNN correctly identified 38 % of the true grave mounds, with 89 % false positives. On a  $937 \text{ km}^2$  area covering Øvre Eiker municipality, Viken County, the R-CNN correctly identified 90 % of the charcoal kilns, with 38 % false positives.

In conclusion, we have demonstrated that Faster R-CNN is well suited for semi-automatic detection of cultural heritage objects such as charcoal kilns, grave mounds and pitfall traps in high resolution airborne lidar data. However, it is desirable to reduce the false positive rate in order to limit the amount of visual inspection needed when the method is applied to large areas for detailed archaeological mapping.

### 1. Introduction

The existing cultural heritage mapping in Norway is incomplete. Some selected areas are mapped well, while the majority of areas only contain chance discoveries, often with bad positional accuracy. The goal of this research was to develop automated tools for improving the cultural heritage mapping in Norway, thus enabling detailed mapping of large areas within realistic budgets and time frames.

All of Norway will soon be covered by ALS data for the purpose of creating a new national elevation model. The Directorate for Cultural Heritage in Norway (Riksantikvaren) wants to use this opportunity to obtain a more complete and accurate mapping of cultural heritage in the

landscape. The highest priority is to map Iron Age grave mounds and ancient deer hunting systems, as these are automatically protected by Norwegian law due to their age, and are also numerous in several parts of Norway. The automatic protection by law applies to such monuments even if they are not yet mapped. There is, however, risk of the monuments being unintentionally destroyed due to lack of knowledge of their existence. It is also desirable to map charcoal kilns, as these occur frequently in some parts of Norway.

Ideally, such a system should satisfy the requirements of

- 1 an automated processing chain,
- 2 reasonable processing time

\* Corresponding author.

E-mail addresses: [trier@nr.no](mailto:trier@nr.no) (Ø.D. Trier), [Jarle.Reksten@nr.no](mailto:Jarle.Reksten@nr.no) (J.H. Reksten), [kristian.loseth@ra.no](mailto:kristian.loseth@ra.no) (K. Løseth).

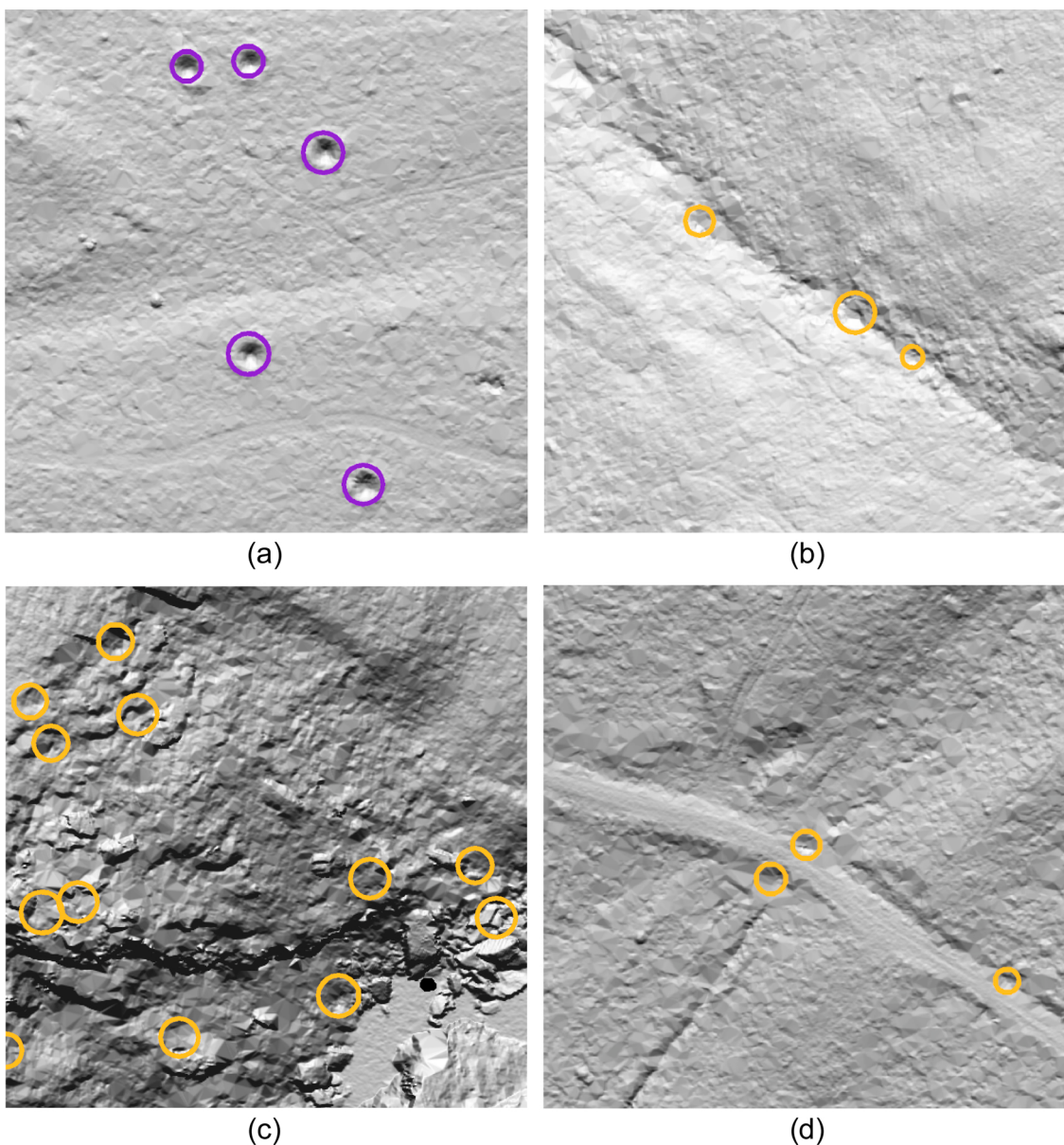


**Fig. 1.** Automatic detections of pit structures using template matching (Trier and Pilø, 2012). Each image portion covers 100m × 100m of terrain, visualized as hillshaded relief of the detailed digital terrain model obtained from the ALS data. Purple circles are archaeological pits, Yellow circles are false positives, i.e., not archaeological structures. (a) Five pitfall traps; image centered on 523,571 east, 6,814,483 north. (b) Three false positives along a creek; image centered on 521,476 east, 6,817,670 north. (c) 12 false positives caused by rough terrain surface including boulders; image centered on 518,965 east, 9,814,490 north. (d) Two false positives at a creek passing under a road, and a false positive at a ditch along a road; image centered on 516,912 east, 6,817,795 north. All coordinates are in UTM zone 32 N. The ALS data was acquired by aircraft on 16 August 2010 with ten points per square meter on average, covering parts of Nord-Fron and Sør-Fron municipalities, Innlandet County. The ALS data may be downloaded from <https://hoydedata.no>, project name Olstappen 2010 (For interpretation of the references to colour in this figure legend, the reader is referred to the web version of this article).

### 3 low numbers of false positives and false negatives 4 applicability to all Norwegian landscapes.

The Norwegian Computing Center has previously developed automated methods for detecting some types of cultural heritage objects from airborne laser scanning (ALS) data (Trier and Pilø, 2012, 2015; Trier et al., 2015a; b; Trier et al., 2018, 2019). These have contributed to increasing the number of areas that are mapped well. However, the methods have a number of issues that have prevented them from being used systematically on all available ALS datasets, as described below.

Trier and Pilø (2012) use template matching to detect pit structures for the purpose of mapping pitfall traps of deer hunting systems and

charcoal burning pits of iron extraction sites. The method works well in areas with relatively smooth terrain surface (Fig. 1a). However, in areas with rough terrain surface, caused by, e.g., creeks (Fig. 1b) or boulder fields (Fig. 1c), a large number of false positives may result. The circular pit template may give a strong response at locations where several points along the edge of the template are higher than in the centre of the template. The response may be higher than at the pit locations that the method is supposed to detect. Also, some modern structures may result in false positives (Fig. 1d).

Trier et al. (2015b) use template matching to detect heap structures for the purpose of detecting Iron Age grave mounds. The method misses some grave mounds but also incorrectly detects a large number of



**Fig. 2.** Grave mounds in Norway's largest Viking Age grave field at Vang, Oppdal municipality, Trøndelag County.



**Fig. 3.** One of the larger grave mounds at Vang, Oppdal, Trøndelag.

natural knolls in the terrain. Despite the limitations of the template matching approach, it has been used in several archaeological mapping projects in Norway (e.g., see: [Trier and Pilø, 2015](#); [Trier et al., 2015a](#)).

[Trier et al. \(2018\)](#) uses a convolutional neural network (CNN) called AlexNet, pre-trained on natural images, followed by a support vector machine classifier to detect charcoal kilns. Compared with template matching, the proposed method achieves better detection performance, both in terms of consumer's accuracy and producer's accuracy. Consumer's accuracy is the ratio of the correctly predicted objects and the true objects. Producer's accuracy is the ratio of the correctly predicted objects and all predicted objects. However, the main problem with the proposed method is that it is very slow. Using a sliding window, the method extracts a small subimage and predicts whether it contains a charcoal kiln or not.

[Trier et al. \(2019\)](#) uses a CNN called ResNet18, also pre-trained on natural images, to detect three types of cultural heritage. The proposed

method produces predictions on a coarse grid, i.e., for each  $32 \times 32$  pixels block in the input image. For two of the three types of cultural heritage, the consumer's accuracy is low.

To summarize, the recent attempts at using deep neural networks ([Trier et al., 2018, 2019](#)) are more successful than template matching, but they still have some drawbacks as mentioned above. Thus, alternative deep neural network were sought. A recent development in deep neural networks for object detection in natural images is the region-proposing convolutional neural network (R-CNN; [Girshick et al., 2014](#)), which may also be used for cultural heritage detection in ALS data. [Verschoof-van der Vaart and Lambers \(2019\)](#) use Faster R-CNN ([Ren et al., 2017](#)) to detect prehistoric barrows and Celtic fields in ALS data from the Netherlands. [He et al. \(2017\)](#) extend Faster R-CNN into Mask R-CNN by providing, for each detected object, an object mask in addition to the bounding box provided by Faster R-CNN. However, as the types of cultural heritage objects in this study were circular, a



**Fig. 4.** Pitfall trap, Innlandet County. Photo: Lars Holger Pilø, Innlandet County Administration.



**Fig. 5.** Charcoal kiln, Lesja, Innlandet County.

bounding box would be sufficient, so an object mask for each detected object would not be necessary. On the other hand, if the types of objects being sought may have different shapes or may be elongated, a predicted object mask would be useful. Then, one may also consider U-Net (Ronneberger et al., 2015), which does semantic segmentation of image data.

## 2. Data

### 2.1. Types of cultural heritage objects

We focus on automated detection of three types of cultural heritage that occur frequently in many types of Norwegian landscape: grave mounds, pitfall traps in deer hunting systems and charcoal kilns.

Grave mounds ([Figs. 2 and 3](#)) are built mainly of earth and are raised over prehistoric graves. Most of the mounds are dated to the Iron Age (ca 500 BC–1000 AD), but in South-East Norway, several grave mounds are dated to ca 1000–1100 AD ([Solberg, 2015](#)). In the Bronze Age burial cairns built of stone were more common. Grave mounds come in many shapes and sizes, the majority being circular. The smallest mounds are just a couple of metres in diameter. Norway's largest burial mound, Raknehaugen, Ullensaker municipality, Viken County, has a diameter of 77 m and is 19 m high. Grave mounds are often found in grave fields containing anything from a couple of graves to several hundreds. The largest grave field in Norway is at Vang, Oppdal municipality, Trøndelag County, with around 900 mounds.

Pits for trapping animals ([Fig. 4](#)) are found all over Norway and were used for hunting large game, especially elk and reindeer (e.g., [Jordhøy](#),

**Table 1**  
ALS datasets used for method development and evaluation.

dataset	ALS project name in hoydedata.no	point density	object type
Larvik 2017	NDH Larvik 5pkt 2017	5/m <sup>2</sup>	grave mound
Horten 2016	NDH Vestfold 5pkt 2016	5/m <sup>2</sup>	grave mound
Hå Jæren 2017	NDH Jæren-Randaberg-Sola 5pkt 2017	5/m <sup>2</sup>	grave mound
Oppdal Vang 2011	Oppdal 12pkt 2011	12/m <sup>2</sup>	grave mound
Sarpsborg 2015	NDH Østfold 5 pkt 2015	5/m <sup>2</sup>	grave mound
Steinkjer 2011	Steinkjer 2011	1/m <sup>2</sup>	grave mound
Steinkjer 2017	NDH Steinkjer 5pkt 2017	5/m <sup>2</sup>	grave mound
Brumunddal 2016	NDH Brumunddal 5pkt 2016	5/m <sup>2</sup>	grave mound
Olstappen 2010	Olstappen 2010	10/m <sup>2</sup>	pitfall trap
Dovre 2011	Dovre 2011	5/m <sup>2</sup>	pitfall trap
Dovre Grimsdalen 2010	Grimsdalen 2010	12/m <sup>2</sup>	pitfall trap
Nordfron 2012	Midt-Gudbrandsdalen 2012	5/m <sup>2</sup>	pitfall trap
Vågå 2018	NDH Vågå-Lom-Skjåk 5pkt 2018	5/m <sup>2</sup>	pitfall trap
Nordfron 2017	NDH Ringebu-Fron-Gausdal 5pkt 2017	5/m <sup>2</sup>	pitfall trap
Nordfron 2018	NDH Ringebu-Fron-Gausdal 5pkt 2018	5/m <sup>2</sup>	pitfall trap
Nordfron Venabu 2018	NDH Venabu 5pkt 2018	5/m <sup>2</sup>	pitfall trap
Dovre 2013	Nord-Gudbrandsdalen 2013	5/m <sup>2</sup>	pitfall trap
Dovre 2017	NDH Lesja-Vågå 5pkt 2017	5/m <sup>2</sup>	pitfall trap
Dovre Foldal 2018	NDH Foldal 5pkt 2018	5/m <sup>2</sup>	pitfall trap
Nordfron 2013	Nord-Gudbrandsdalen 2013	5/m <sup>2</sup>	pitfall trap
Lesja 2013	Nord-Gudbrandsdalen 2013	5/m <sup>2</sup>	charcoal kiln

**Table 2**  
ALS datasets used for new archaeological mapping.

dataset	ALS project name in hoydedata.no	point density
Øvre Eiker 2015	Drammen Eiker 2015	5/m <sup>2</sup>
Øvre Eiker Flesberg 2017	NDH Flesberg-Rollag-Øvre Eiker 5pkt 2017	5/m <sup>2</sup>
Øvre Eiker Modum 2017	NDH Modum-Sigdal 5pkt 2017	5/m <sup>2</sup>

2008). The earliest traps found are dated to the Stone Age but most of the pits found were used in the period 1–1350 AD. There was still some hunting with pitfall traps in the 18th century. The pits are usually around 4–7 m in diameter with a depth of 2 m.

Charcoal kilns (Fig. 5) are found several places in Norway, especially places related to production of metal and metalworking. In these kilns charcoal was produced by placing wood in a circular pile and covered with turf and dirt. After burning the charcoal was extracted leaving behind a distinctive platform which usually has a diameter of 10–20 m. This technology for producing charcoal was introduced in the second half of the 16th century. The use of charcoal kilns was greatly reduced after 1860. The charcoal kilns may have varied topographical expressions. Some kilns have a surrounding circular ditch, some have pits along their circumference, and some have a combination of the two. Additionally, some kilns have a low mound inside the ditch/pits, while some have pits inside the circumference (Trier et al., 2018).

The current mapping in Norway of cultural heritage, including the three types described above, is in the form of a national cultural heritage

database named Askeladden. A search and view functionality into this database is available to the public at <https://kulturminnesok.no/>. The majority of the contents of this database are the results of surveys and registrations conducted by the cultural heritage administrations at the county level and the national level. Only occasionally has this work led to scientific publications.

## 2.2. Airborne laser scanning data

ALS point cloud datasets (Tables 1 and 2) were downloaded from <http://hoydedata.no>. This internet site provides free access to all ALS data in Norway. All the ALS datasets (Tables 1 and 2) are located in Southern Norway (Fig. 6).

For all the ALS datasets in Table 1, vector maps of known locations of grave mounds, pitfall traps and charcoal kilns were provided as ESRI shape files. The vector maps of grave mounds and pitfall traps were provided by the Directorate for Cultural Heritage in Norway. These data were extracted from the national cultural heritage database. The vector maps of charcoal kiln locations were provided by Innlandet County Administration. None of the vector maps are freely available.

All the vector data were visually checked against visualizations of the ALS data. Both hillshade visualizations and local relief model visualizations were used. The purpose was to ensure that the vector data agreed with the visual appearance of objects in the ALS data, to ensure the neural network learned the shapes of the cultural heritage objects. This was considered necessary in order to obtain reduced rates of false positives and false negatives, compared to previous methods that have been used (Trier and Pilø, 2012, 2015; Trier et al., 2015a, b; Trier et al., 2018, 2019). For objects not clearly visible in the ALS data, the vector outlines were removed. Inaccurate vector outlines were corrected to match the visible object boundaries in the ALS data. Also, missing vector outlines were added. For the Oppdal Vang 2011 dataset, small grave mounds were removed from the vector data. These small grave mounds were not considered to be representative for grave mounds in the other ALS datasets.

On a few occasions, documented grave mounds are removed. At Søndre Kaupang (Fig. 7) eight removed grave mounds are discovered in an agricultural field in 2016 using ground penetrating radar, by Christer Tonning, Vestfold and Telemark County Administration. Since the grave mounds are not visible in the ALS data, the outlines of the eight grave mounds were removed from the vector data. At Ommundrød (Fig. 8a,c) a grave mound is removed due to road construction. At Manvik, a house is replacing a grave mound (Fig. 8b,d). In all such cases, the outlines of the removed grave mounds were deleted from the vector data. On several occasions, individual grave mounds were difficult to see in the ALS data (Fig. 9), and were thus removed from the vector data.

For grave mounds that were clearly visible in the ALS data, the vector outlines were adjusted to match the ALS data, as in the following examples (Fig. 10). At Kleppaker øvre (Fig. 10a) the existing grave mound outlines were moved and enlarged to match the ALS data, and a missing grave mound outline was added. At Nedre Håvet (Fig. 10b), one grave mound outline was deleted, since the grave mound was difficult to see in the ALS data. The three remaining grave mound outlines were moved and enlarged to match the ALS data. At Sanden vestre (Fig. 10c), the existing grave mound outlines (cyan) are correctly centred, but were enlarged (purple) to include the entire shape of each grave mound. Two grave mound outlines were removed as the grave mounds were not clearly visible in the ALS data.

For some grave fields, many of the individual grave mounds are flat and thus difficult to see clearly in the ALS data. E.g., at Lamøya grave field (Fig. 11), only 25 of 93 grave mound contours were kept. For several other grave fields, the individual grave mounds are not mapped. In these cases, for each grave mound clearly visible in the ALS data, a vector outline was added (Fig. 12). Often, some of the grave mounds are outside the previously mapped grave field boundary, meaning that the existing mapping may be misleading in land use planning.

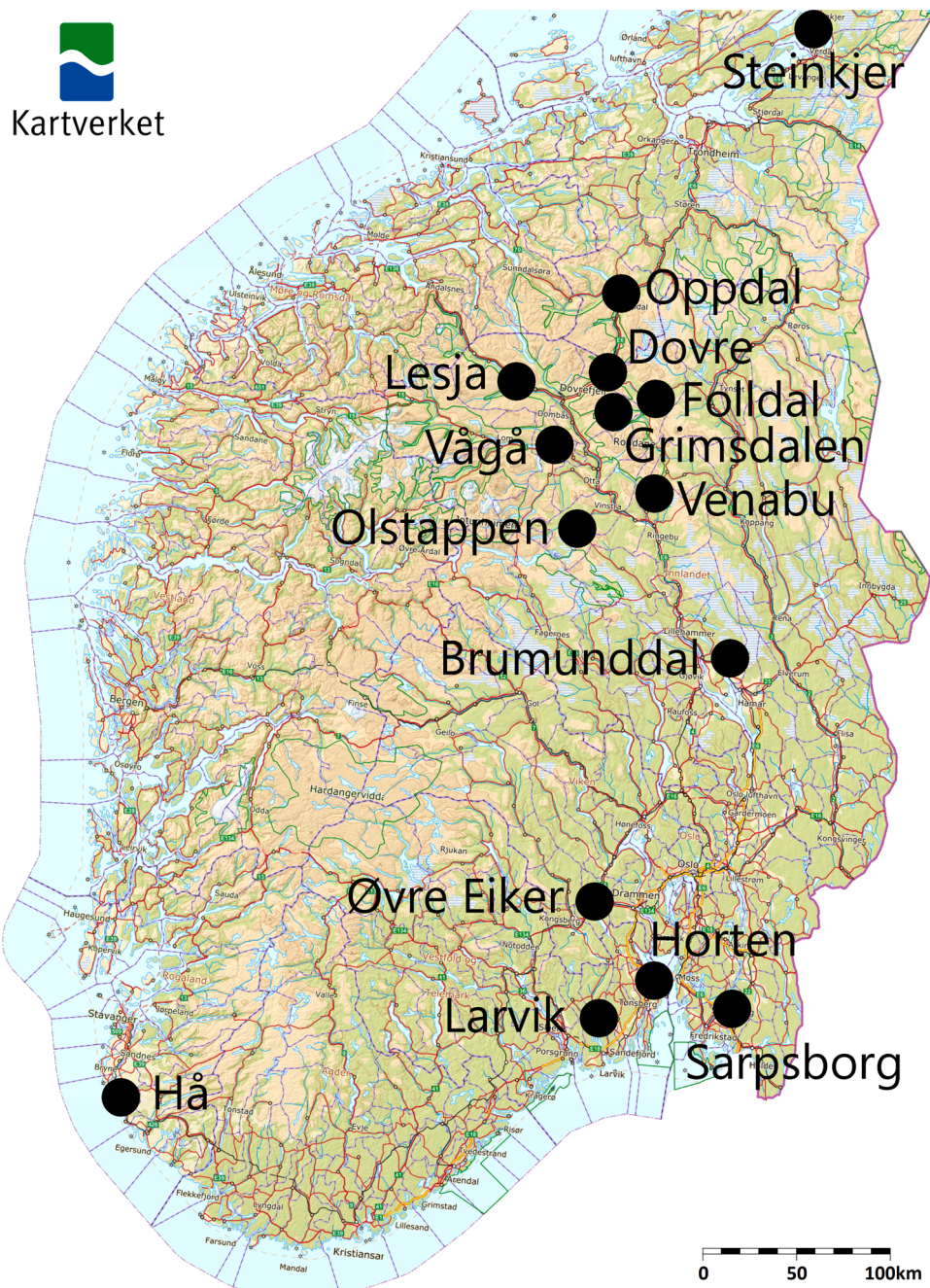


**Fig. 6.** The locations of the various ALS datasets. Topographic map of Southern Norway from <https://hoydedata.no>, the Norwegian Mapping Authority (Kartverket).

With the vector outlines collected so far, the neural network was trained and then run on the Larvik data to detect any missing grave mounds. The vector outlines of possible grave mounds were visually checked in the ALS data, keeping only the ones that clearly looked like grave mounds (Fig. 13).

The ALS datasets in Table 2 were selected to cover Øvre Eiker municipality, Viken County. Øvre Eiker had a low number of known cultural heritage object locations, but had potential for a large number of previously unknown charcoal kilns. The nearby Kongsberg silver works (1623–1958) had a huge demand for charcoal until dynamite and electricity was available. There was also local interest in the municipality administration for detailed archaeological mapping. Combined, the three ALS datasets cover the entire area of the municipality.

### 2.3. Subdivision of labelled data into training, validation and test

The data in Table 1 were split into three parts, named ‘training’, ‘validation’, and ‘test’ (Table 3). The neural network parameters would be learned from the training data iteratively by minimising a loss function. The validation data would be used to select the best set of neural network parameters. The test data would then be used to estimate detection performance on data not seen during training.

On average, 54 %, 29 % and 17 % of the known objects were included in the training, validation and test sets, respectively (Table 4). One purpose of the splitting was to obtain realistic estimates on how the detection performance may be on unlabelled ALS datasets, which is the expected situation when performing detailed archaeological mapping.

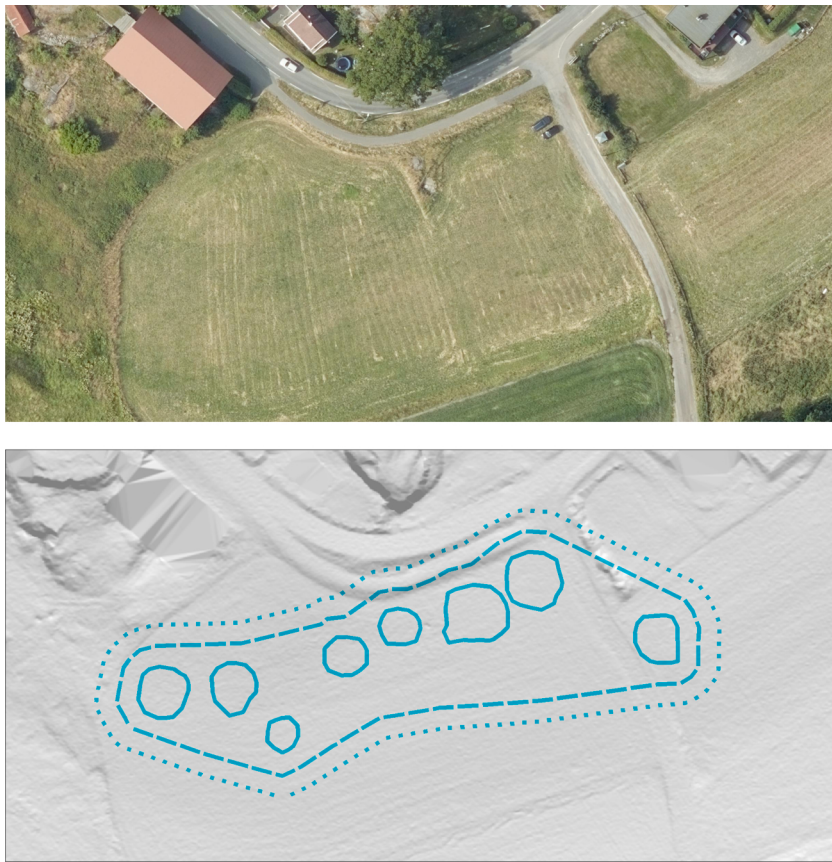


**Fig. 7.** A grave field at Søndre Kaupang, Larvik municipality, Vestfold and Telemark County, was discovered using ground penetrating radar in 2016. The grave mounds have been removed and the grave field is now part of an agricultural field. Top: air photo of 20 July 2017. Bottom: hillshade visualization of ALS data (grey), remains of grave mounds (cyan solid outlines) mapped using ground penetrating radar, grave field extent (dashed cyan line) and precaution zone (dotted cyan outline). The area shown covers 200 m × 100 m, centered on coordinates 218,750 east, 6,553,905 north, UTM zone 33 N.

Another purpose was to obtain a sufficient amount of representative training data for tuning of the parameters of the deep neural network. A third purpose was to reduce the chances of overfitting of the neural network parameters. Overfitting means that the neural network performs well on data that are similar to the training data but performs poorly on other data.

#### 2.4. Unlabelled test data

The three unlabelled lidar data sets covering Øvre Eiker municipality (Table 2) consists of 1493 LAS files in total (Table 5).

### 3. Methods

#### 3.1. Preprocessing

The ALS point cloud data were converted to a digital terrain model (DTM) with 0.25 m pixel spacing. The DTM was converted to a simplified local relief model (LRM) by subtracting a smoothed version of the DTM: For each pixel, the average within a  $31 \times 31$  pixels ( $7.75 \text{ m} \times 7.75 \text{ m}$ ) window centred on the pixel was used as the smoothed value. The LRM enhances local elevation differences while suppressing the general landscape topography (Hesse, 2010). Thus, cultural heritage objects including grave mounds, pitfall traps and charcoal kilns may be visible. The simplified local relief model is faster to compute than the complete local relief model, while the visibility of the cultural heritage objects remains.

For each cultural heritage object in the vector data, a  $150 \text{ m} \times 150 \text{ m}$  image was extracted from the LRM. The object's position within the

subimage was selected at random. This was done in order to prevent the deep neural network from always predicting the object in the image centre. All cultural heritage objects within the subimage were included in the image annotation. Thus, each image contained one or more clearly visible cultural heritage objects.

#### 3.2. Data augmentation

For each of the extracted images in the training and validation subsets, eight different versions were made by rotating the image by 0, 90, 180 and 270 degrees, and by creating mirrored versions of all four rotations. In this way, the number of training and validation images were increased by a factor of eight, thus creating more variability in the dataset without the need for more labelled examples of cultural heritage objects. An underlying assumption was that neither the cultural heritage objects nor the landscape topography had any preferred orientation for their structures. However, for the extracted images in the test subset, no extra versions were made (Table 6).

In fact, even more augmentations could have been made by allowing rotation by any angle in the range 0–360 degrees and not only multiples of 90 degrees. However, the number of training and validation images obtained with four rotations and mirroring (Table 6) were considered sufficient.

One may observe that the number of images (before augmentation) are higher than the corresponding number of objects. The number of objects are from the vector files, and count the number of objects that are inside each lidar dataset extent. However, the raster images of  $600 \times 600$  pixels were extracted from LRM files with some overlap. Thus, one vector object near an LRM file boundary may be included in more than

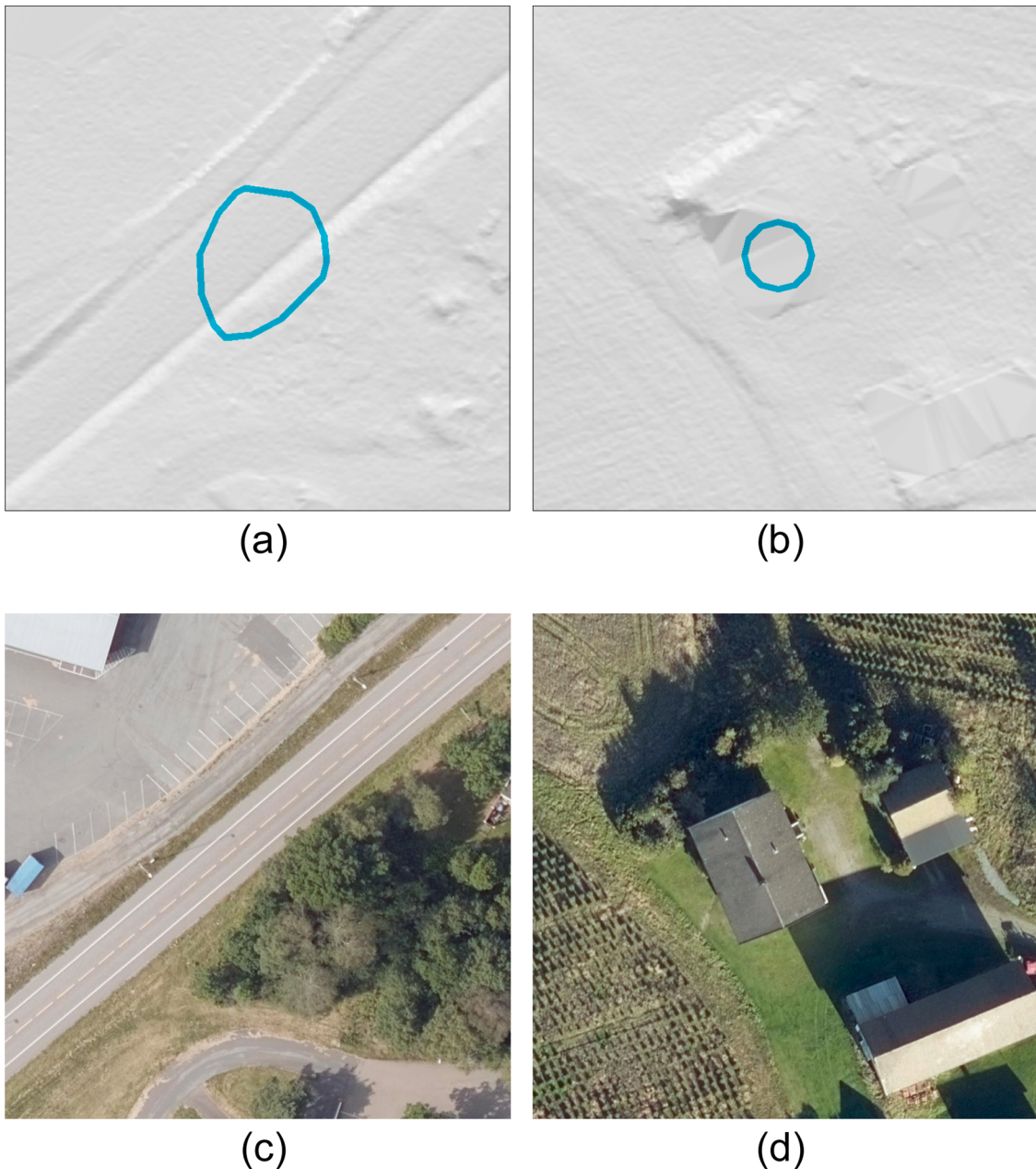


**Fig. 8.** Two locations in Larvik municipality, Vestfold and Telemark County, where grave mounds are removed. Each image covers a 75 m × 75 m area; coordinates are in UTM zone 33 N. Top row: ALS hillshade visualizations with grave mound locations (cyan solid outline). Bottom row: Air photos of the same areas. (a) A grave mound at Ommundrød is excavated and removed in 1955 due to road construction; location: 220,100 east, 6,562,008 north. (b) At Manvik, a house is at the location of a previous grave mound; location: 208,674 east, 6,550,043 north. (c) Air photo of 20 July 2017. (d) Air photo of 6 October 2017.

one LRM file, thus resulting in more than one extracted raster image.

### 3.3. Detection

For detection, the Python code library *simple faster R-CNN* was downloaded from <https://github.com/chenyuntc/simple-faster-rnn-pytorch>. For each detected object, the R-CNN predicts a bounding box, a class label and a score value in the range 0.0 – 1.0. Pre-training of the neural network was done by importing parameters learned from the VGG16 deep neural network (Simonyan and Zisserman, 2015) on the ImageNet dataset of photographs with labelled objects such as cars, dogs, etc. (Russakovsky et al., 2015). A file with the parameters learned from this pre-training came with the downloaded source code.

A few modifications had to be done:

- 1 The list of class labels was changed to match the class labels used in the image annotations.
- 2 Additional training was done on annotated LRM images containing cultural heritage objects.
- 3 The downloaded code crashed if there were no detected objects within an image. Thus, if-tests had to be added.

When these changes were made, the Python code predicted the locations and sizes of grave mounds (Fig. 15), pitfall traps (Fig. 16) and charcoal kilns (Fig. 17) in LRM images of size 600 × 600 pixels (150 m × 150 m). A score value between 0.0 and 1.0 was given for each predicted

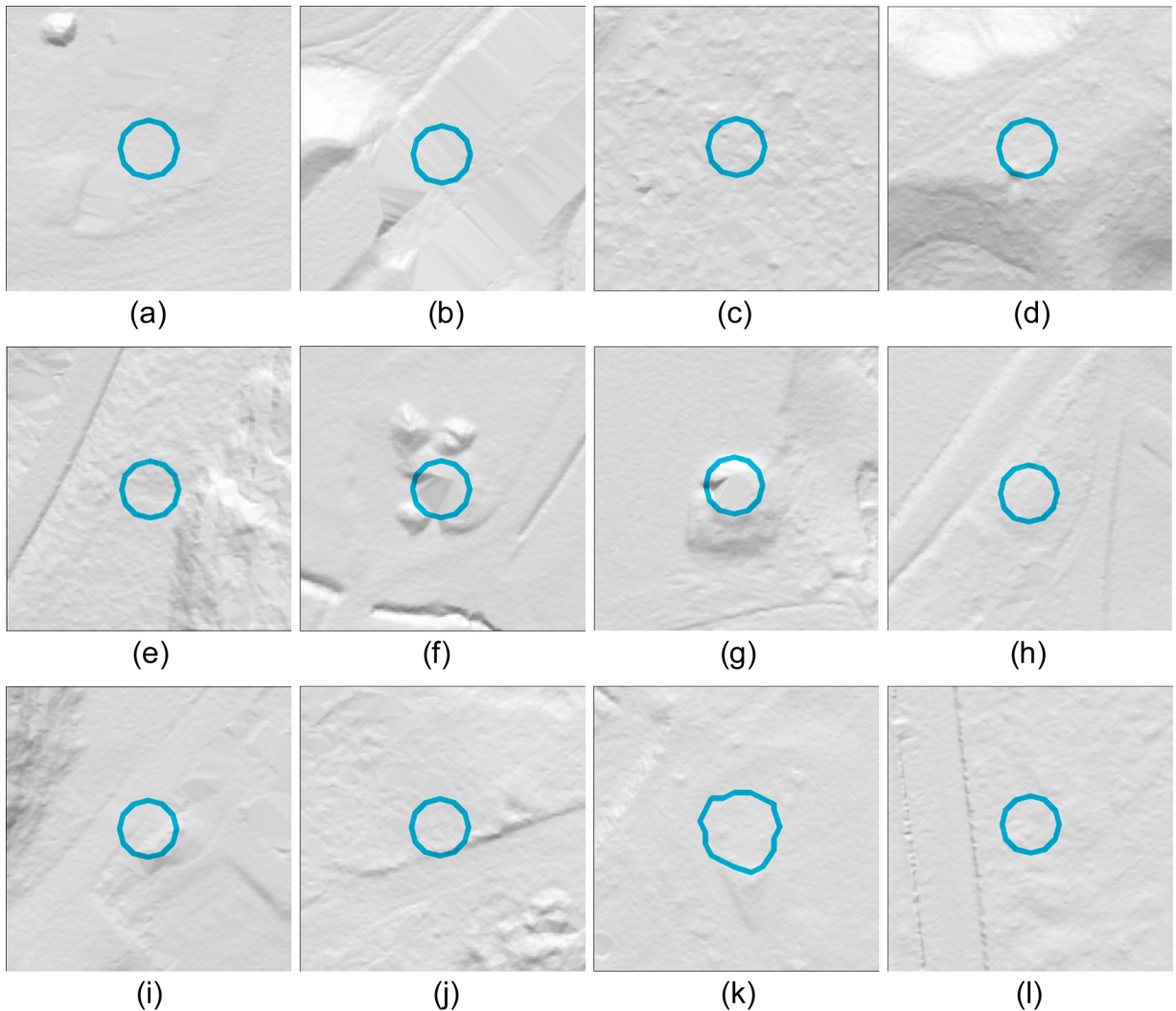


**Fig. 9.** Some locations in Larvik municipality, where grave mound shapes were difficult to see in the ALS data. Each ALS hillshade image covers a 50 m × 50 m area; coordinates are in UTM zone 33 N. (a) At Kamperhaug (207,902 east, 6,552,326 north), there was no visible trace of the grave mound in the ALS data. (b) At Rødbøl (219,332 east, 6,561,718 north), there is now a motorway bridge, so the ground surface was not visible in the ALS data. (c) Southwest of Solberg (208,777 east, 6,553,748 north), for a grave mound in a forest, there was no visible trace of the grave mound in the ALS data. (d) At Sanden vestre (208,288 east, 6,551,936 north), a grave mound with a looting pit, centered on the southern edge of the vector outline (cyan) was slightly visible in the ALS data. (e) At Hyatum østre (210,440 east, 6,552,686 north), a grave mound was slightly visible in the ALS data, centered on the northeastern edge of the vector outline (cyan). (f) At Kolbensrød (211,060 east, 6,549,542 north), there is a house at the grave mound vector outline (cyan). The two heaps on the northern side are modern piles of gravel, and the heap on the southwestern side looks like a modern pile of soil. (g) At Foldvik østre (211,347 east, 6,550,083 north), there is missing ALS data in the centre of the grave mound, distorting the grave mound shape in the ALS data. (h) At Linnum (211,596 east, 6,552,309 north), a flat grave mound was difficult to see in the ALS data. (i) At Tanum prestegård (211,560 east, 6,553,731 north), the mound appeared as partly removed in the ALS data. (j) At Ulleberg, in the ALS data, there seemed to be a grave mound (at 212,252 east, 6,553,661 north) 12 m east of the cyan vector outline (at 212,240 east, 6,553,658 north). The grave mound seemed to be damaged at the southern edge due to a dirt road. (k) At Agnes (214,909 east, 6,552,285 north), there is no visible grave mound in the ALS data. However, 60 m to the south, there is a location that matches the textual description “grave mound at the centre of a roundabout”, but the grave mound was not clearly visible in the ALS data at that location. (l) At Mellomskogen (215,000 east, 6,557,114 north), there was no visible grave mound in the ALS data. However, 40 m to the north, there was a structure in the ALS data that might be a grave mound.

object. Objects with a score value below 0.7 were discarded by the automatic method.

#### 3.4. Processing chain

The pre-processing and detection methods were integrated into a Python script (Fig. 14) that may be called from QGIS or started from the Linux command line. The input was a collection of LAS files, and the output was two ESRI shape files for each object type; centre points in one file and object outlines in another file. Each object outline was obtained by converting the predicted bounding box to a circle.

## 4. Results

The detection results (Table 7) were obtained by running the method on 737 test images not seen during training. Each test image contained one or more cultural heritage objects, and 597 unique cultural heritage objects in total. All in all, the test images contained 2144 cultural heritage objects including duplicates. 87 % of the true cultural heritage objects were detected with the correct class (consumer's accuracy). Less than 1 % of the cultural heritage objects were detected with the wrong class, while 13 % of the cultural heritage objects were not detected.

Of the 2466 predicted cultural heritage objects, 75 % were predicted

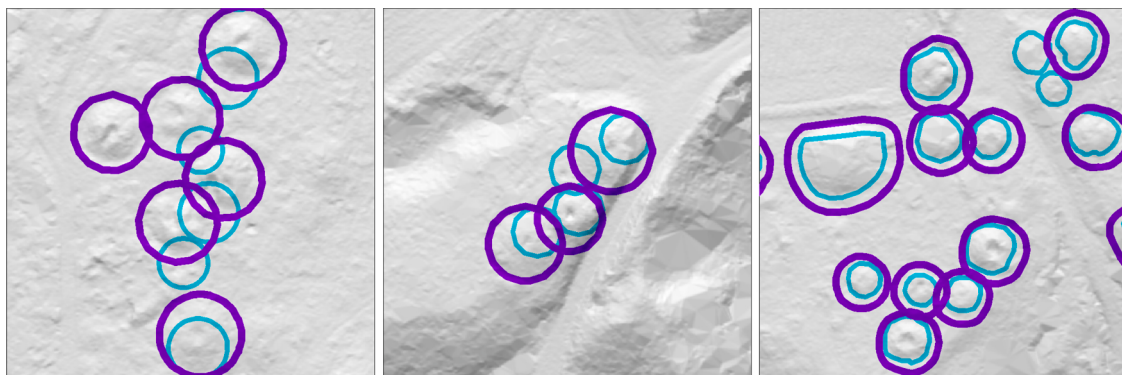


**Fig. 10.** Existing grave mound outlines (cyan circles) were corrected (purple circles) in the vector data for several locations in Larvik municipality. Each ALS hillshade image covers a 75 m × 75 m area. (a) Grave field at Kleppaker øvre; location: 224,783 east, 6 557,045 north, UTM zone 33 N. (b) Grave field at Nedre Håvet; location: 213,273 east, 6,592,819 north, UTM zone 33 N. (c) Grave field at Sanden vestre; location: 208,422 east, 6,551,938 north, UTM zone 33 N (For interpretation of the references to colour in this figure legend, the reader is referred to the web version of this article).

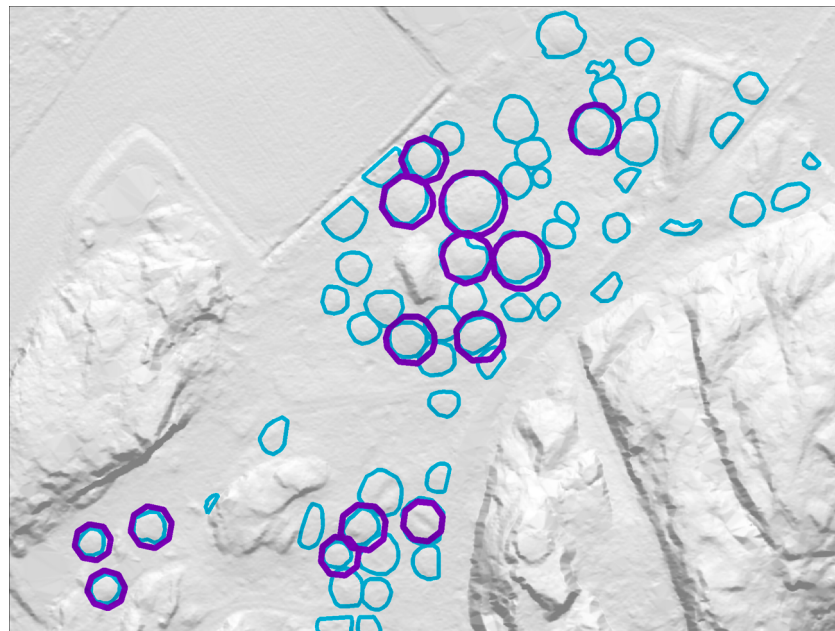


**Fig. 11.** The middle part of Lamøya grave field. Cyan: outlines of all grave mounds. Purple: edited outlines of grave mounds clearly visible in the ALS data. The ALS hillshade image covers 200 m × 150 m, centered on 219,387 east, 6,553,851 north, UTM zone 33 N (For interpretation of the references to colour in this figure legend, the reader is referred to the web version of this article).

with the correct class (producer's accuracy), while 24 % of the predicted objects were false positives (background). However, there were no images without cultural heritage objects. Thus, the reported number of false positives (24 %) may be too optimistic an estimate for a large landscape.

In order to estimate how well the automated method was for obtaining a complete mapping, annotated data were prepared for the Larvik test area ( $67 \text{ km}^2$ ). For this area, all grave mound and grave field locations from the Askeladden national cultural heritage database were included. As noted above, some of the grave fields were missing individual grave mound locations. These were added manually, in part by identifying the locations in the LRM and/or hillshade visualizations (Fig. 12), and in part by studying the textual descriptions of the grave field. In several cases, the grave field descriptions included descriptions of the locations of the individual grave mounds. For any grave mound location that was predicted by the automatic method but missing in the

Askeladden database, a visual inspection of the LRM and hillshade visualizations was done. If the grave mound location was confirmed by the visual inspection, then it was included in the annotated vector data (Fig. 13).

The automatic method was able to correctly identify 38 % of the true grave mound locations, thus missing 62 % of the grave mounds (Table 8). However, some of these have been removed, while others were difficult to see in the LRM and hillshade visualizations. Thus, there were two sources of missing grave mounds in the automatic detection results: (1) the grave mounds were not visible in the visualizations of the lidar data, which was a limitation of this data type, and (2) the automatic method was missing some grave mounds even if they were visible in the visualizations of the lidar data.

Another effect of applying the automatic method on an entire area was that the false positive rate increased, or, in other words, the producer's accuracy was reduced. For the Larvik test area, the producer's

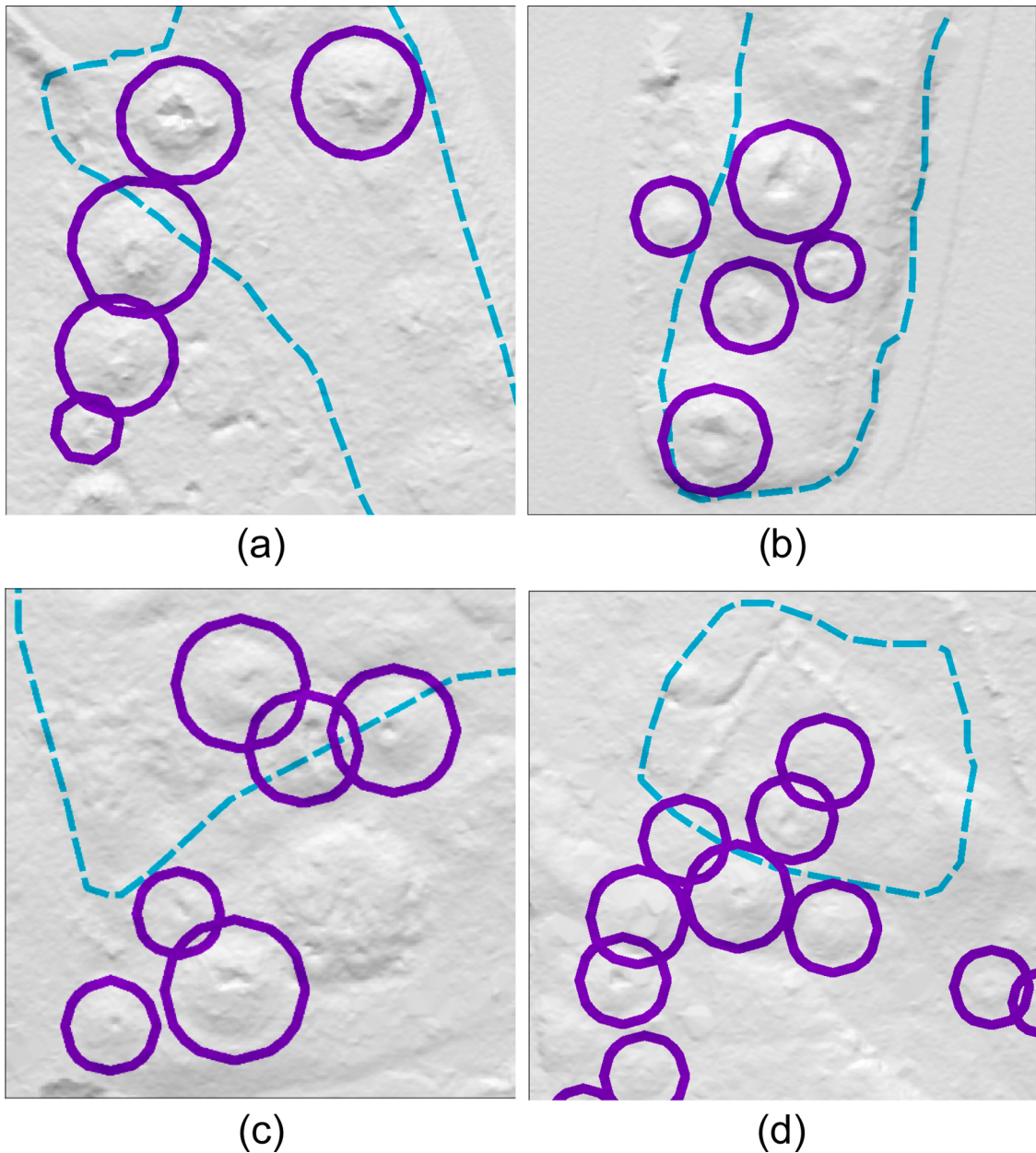


**Fig. 12.** Grave fields (cyan dashed outlines) lacking mapping of individual grave mounds. Outlines (purple) were added for the grave mounds clearly visible in the ALS data. Each ALS hillshade image covers 75 m × 75 m; coordinates are in UTM zone 33 N. (a) Lunde sørde, location: 217,392 east, 6,563,150 north. (b) Landhjem, location: 217,456 east, 6,561,595 north. (c) Ulleberg, location: 212,317 east, 6,554,419 north. (d) Gui nedre, location: 209,214 east, 6,552,130 north (For interpretation of the references to colour in this figure legend, the reader is referred to the web version of this article).

accuracy for grave mounds was 14 %, meaning that only 14 % of the predicted grave mounds were in fact grave mounds. In other words, 86 % of the predicted grave mounds were in fact not grave mounds. By also including false detections of charcoal kilns and pitfall traps, the producer's accuracy was 11 %.

The method was then used on all of Øvre Eiker municipality, an area with few recorded charcoal kilns; thus, no ground truth existed. This is the normal situation for the practical use of the method, in order to discover previously unknown cultural heritage locations. 1130 charcoal locations were predicted by the method (Table 9, Fig. 18). All of these were checked manually by visual inspection of the LRM visualizations of the ALS data. In this way, 51 % were confirmed as being charcoal kilns (e.g., Fig. 19), while another 11 % appeared to be possible charcoal kilns. By including confirmed and possible charcoal kilns, the producer's

accuracy was estimated to be 62 %. During the visual inspection, charcoal locations missing automatic prediction were identified. 66 such locations were visually confirmed. By counting only the visually confirmed charcoal kiln locations, the consumer's accuracy was estimated to be 90 %.

## 5. Discussion and conclusions

The classification performance of the automatic method varied between the three test scenarios. The first test scenario, with all 150 m × 150 m test images containing at least one cultural heritage object, gave a false positive rate of 24 %. This increased to 89 % when the method was applied on the full area of the Larvik test set ( $67 \text{ km}^2$ ) and to 38 % on the Øvre Eiker test set ( $937 \text{ km}^2$ ). Thus, the false positive rate in the first test

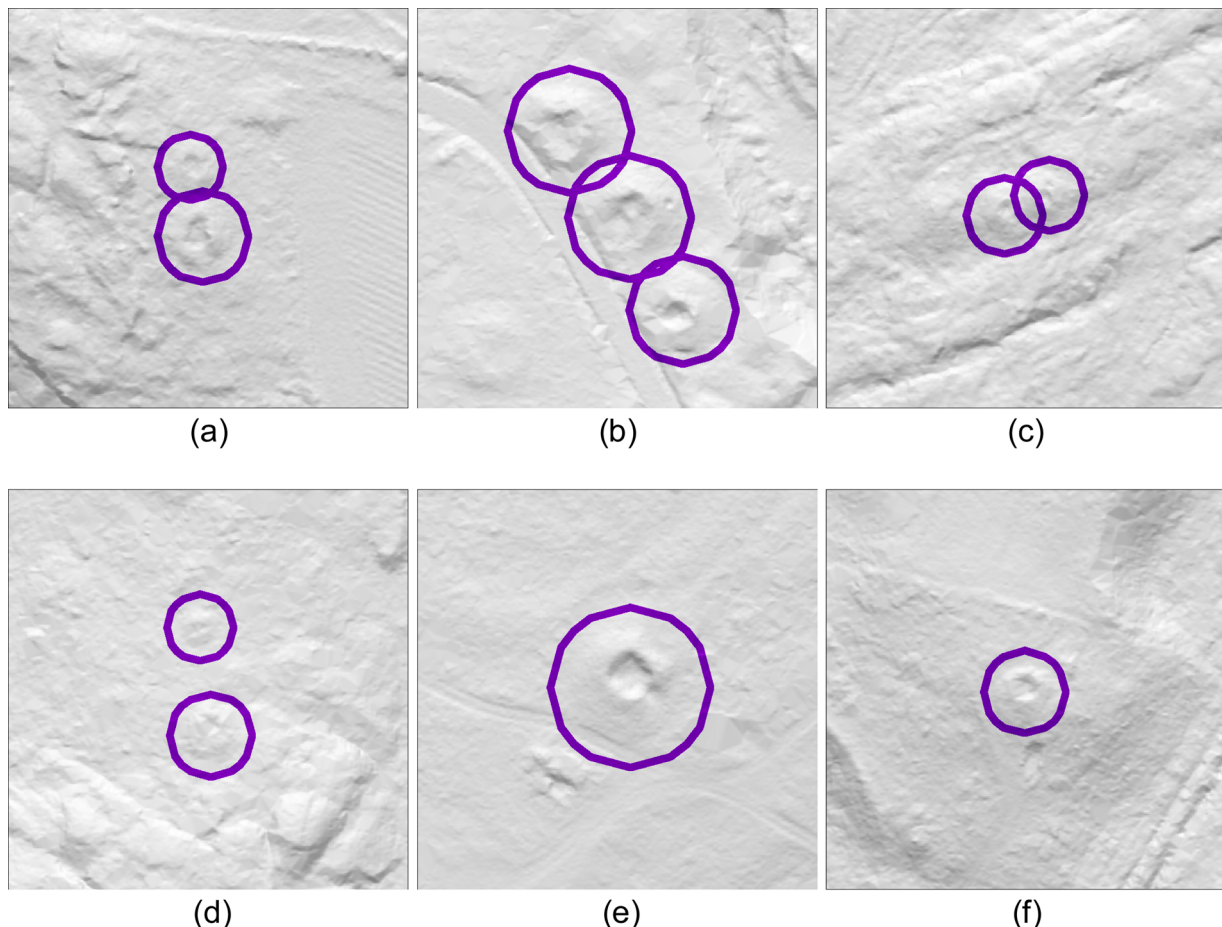


**Fig. 13.** Grave mounds detected and added to the vector data. Each ALS hillshade image covers 75 m × 75 m; coordinates are in UTM zone 33 N. (a) Location: 209,073 east, 6,552,295. (b) Location: 208,650 east, 6,551,759 north. (c) Location: 206,727 east, 6,547,916 north. (d) Location: 209,254 east, 6,549,298 north. (e) Location: 206,802 east, 6,550,326 north. (f) Location: 213,559 east, 6,592,854 north.

scenario was too optimistic. The differences in false positive rates between Larvik and Øvre Eiker are in part because detection was evaluated for three types of cultural heritage objects for Larvik, but only charcoal kiln detection was evaluated for Øvre Eiker. For Larvik, 41 out of 813 false positives were predicted as charcoal kilns, while 610 were predicted as grave mounds. This indicates that, compared to charcoal kilns, grave mounds are more easily confused with natural terrain features and/or modern terrain modifications visible in the image data.

The true positive rate also varied between the three test scenarios. The first test scenario gave a true positive rate of 87 % overall, with 84 % for grave mounds and 96 % for charcoal kilns. Compared to charcoal kiln detection on the Øvre Eiker test set, the true positive rate dropped slightly, from 96 % to 90 %. However, for grave mound detection, the true positive rate dropped dramatically from 84 % on the first test scenario to 38 % on the Larvik test set. The main reason was that the number of grave mounds in the ground truth data for the Larvik test area had increased from 57 to 269, thus including a large number of grave mounds that were difficult to see in the LRM visualizations of the lidar data. This drop in true positive rate indicates three things. First, the automatic method is good at detecting objects clearly visible in the image data, provided it has been trained on images with similar objects. Second, the automatic method is less successful at providing a complete archaeological mapping of the selected cultural heritage objects if these

are not always clearly visible in the image data. Third, there is a potential for better true positive rates by including objects not clearly visible in the training data, albeit at the risk of increasing the false positive rate.

Despite these imperfections, the method has been used at the Directorate for Cultural Heritage in Norway on a number of ALS datasets covering a variety of landscape types, including forest, mountain, urban, rural, agricultural and coastal areas. Although a detailed quantification of detection performance has not yet been performed, as it is very time consuming, some trends were observed through practical use of the method for detailed archaeological mapping. The method performed better on charcoal kilns than on the other object types. In the inland, the method performed well on pitfall traps. This included many areas that are lacking detailed cultural heritage mapping. An unexpected result was that charcoal pits / tar pits were detected, albeit as pitfall traps. Thus, the automatic method was able to detect a type of cultural heritage object not seen during training, but confused it with another type due to the similarities in their appearances in the LRM visualizations. For grave mounds, the method was less successful. Confusion between natural knolls and grave mounds was the main problem. Still, the method may be useful by giving an overview of locations in the landscape with structures resembling grave mounds. These could then be checked visually by an experienced archaeologist, who could spot which

**Table 3**

Subdivision of ALS datasets into training, validation and test sets.

object type	dataset	subset	object count	extent of dataset in UTM zone 33 N				area km <sup>2</sup>
				west	east	south	north	
charcoal kiln	Lesja 2013	training	773	160,750	172,000	6,907,150	6,919,600	140
		validation	190	154,350	172,000	6,902,500	6,919,600	302
		test	95	144,800	154,400	6,916,000	6,922,800	65
grave mound	Brumunddal 2016	validation	23	260,000	280,000	6,753,600	6,774,600	420
		test	50	269,600	283,200	6,736,200	6,753,000	228
grave mound	Horten 2016	training	38	238,400	243,200	6,588,000	6,593,400	26
grave mound	Hå Jæren 2017	validation	84	-44,000	-36,000	6,531,800	6,545,400	109
grave mound	Larvik 2017	training	288	206,400	220,800	6,547,800	6,563,400	225
		validation	165	205,600	218,400	6,565,800	6,596,400	392
		test	57	220,800	226,400	6,553,200	6,565,200	67
grave mound	Oppdal Vang 2011	training	219	224,690	225,600	6,951,850	6,952,925	1.0
grave mound	Sarpsborg 2015	validation	30	274,400	280,000	6,576,000	6,583,800	44
grave mound	Steinkjer 2011	test	18	276,000	284,800	6,565,200	6,575,400	90
grave mound	Steinkjer 2017	test	44	321,600	348,800	7,087,800	7,113,000	685
pitfall trap	Dovre 2011	training	368	199,200	218,400	6,902,400	6,915,000	242
		validation	282	192,000	206,400	6,885,600	6,902,400	242
pitfall trap	Dovre 2013	test	29	190,400	204,000	6,878,400	6,897,000	253
pitfall trap	Dovre 2017	test	15	190,400	196,800	6,882,000	6,897,000	96
pitfall trap	Dovre Folldal 2018	test	3	233,600	234,400	6,891,600	6,892,200	0.5
pitfall trap	Dovre Grims-dalen 2010	test	155	219,200	231,200	6,893,400	6,899,400	72
pitfall trap	Nordfron 2012	training	31	202,800	206,400	6,837,000	6,839,400	8.6
		validation	18	221,600	226,400	6,835,800	6,848,400	60
		test	31	200,800	219,200	6,833,400	6,840,600	132
pitfall trap	Nordfron 2013	training	25	191,200	193,600	6,831,000	6,832,200	2.9
pitfall trap	Nordfron 2017	test	6	193,600	194,400	6,831,000	6,832,200	1.0
pitfall trap	Nordfron 2018	training	3	220,000	221,600	6,841,800	6,842,400	1.0
		validation	12	220,800	224,800	6,837,600	6,839,400	7.2
		test	1	211,200	212,000	6,831,000	6,831,600	0.5
pitfall trap	Nordfron 2018	training	48	210,400	212,000	6,837,000	6,839,400	3.8
		validation	152	196,800	200,000	6,825,000	6,827,400	7.7
		test 1	6	208,800	210,400	6,841,200	6,841,800	1.0
pitfall trap	Nordfron Olstappen 2010	test 2	9	197,600	199,200	6,821,400	6,822,600	1.9
		training	68	195,470	202,400	6,827,400	6,830,400	21
		validation	57	200,800	204,800	6,826,400	6,828,000	6.4
pitfall trap	Nordfron Venabu 2018	test	41	195,200	202,400	6,830,400	6,832,200	13
		validation	10	222,400	224,000	6,861,000	6,862,200	1.9
pitfall trap	Vågå 2018	test	7	224,000	227,200	6,844,800	6,858,600	44
		training	70	184,000	188,800	6,849,650	6,862,800	63
		validation	34	171,200	180,700	6,832,800	6,847,200	137

**Table 4**

Summary of ALS data used for neural network training and evaluation.

object type	number of objects				sum		
	training	validation	test	sum			
charcoal kiln	773	73 %	190	18 %	95	9 %	1058
grave mound	545	52 %	302	29 %	199	19 %	1046
pitfall trap	613	41 %	565	38 %	303	20 %	1481
sum	1931	54 %	1057	29 %	597	17 %	3585

**Table 5**

Extent of the ALS datasets covering Øvre Eiker municipality.

dataset	extent of dataset in UTM zone 32 N				number of files	area km <sup>2</sup>
	west	east	south	north		
Øvre Eiker 2015	537,600	556,000	6,609,600	6,640,800	494	574
Øvre Eiker Flesberg 2017	535,200	556,800	6,604,800	6,642,600	829	816
Øvre Eiker Modum 2017	550,400	560,000	6,626,400	6,639,000	170	121
Combined	535,200	560,000	6,604,800	6,642,600	1,493	937

**Table 6**

The number of extracted images for the training, validation and test subsets.

object type	number of objects				number of images, no augmentation				number of images, with augmentations	
	training	validation	test	sum	training	validation	test	sum	training	validation
charcoal kiln	773	190	95	1,058	907	230	110	1,247	7,256	1,840
grave mound	545	302	199	1,046	616	359	248	1,223	4,928	2,872
pitfall trap	613	565	303	1,481	774	682	379	1,835	6,192	5,456
sum	1,931	1,057	597	3,585	2,297	1,271	737	4,305	18,376	10,168

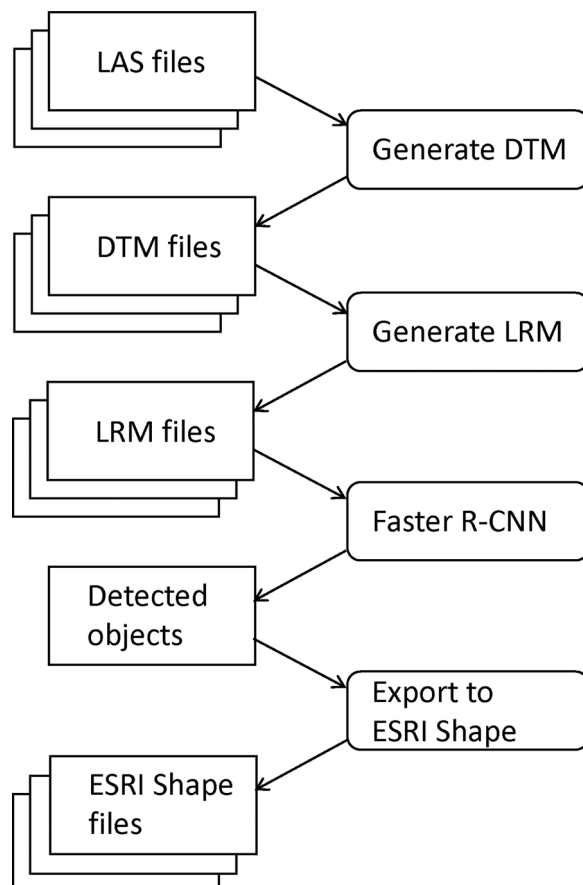


Fig. 14. Processing steps (rounded boxes) and data units (rectangles) in the Python processing chain.

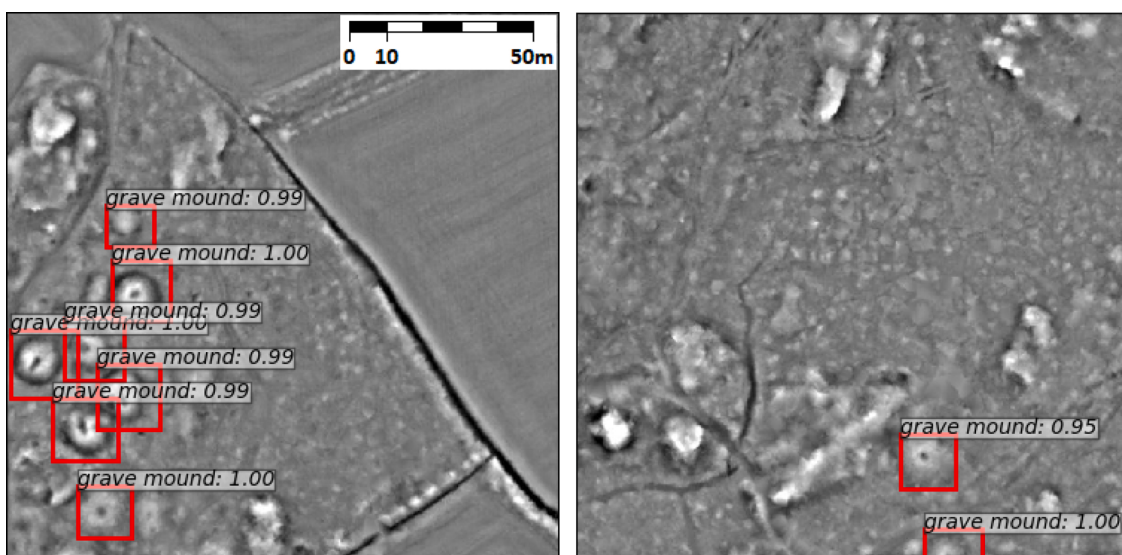
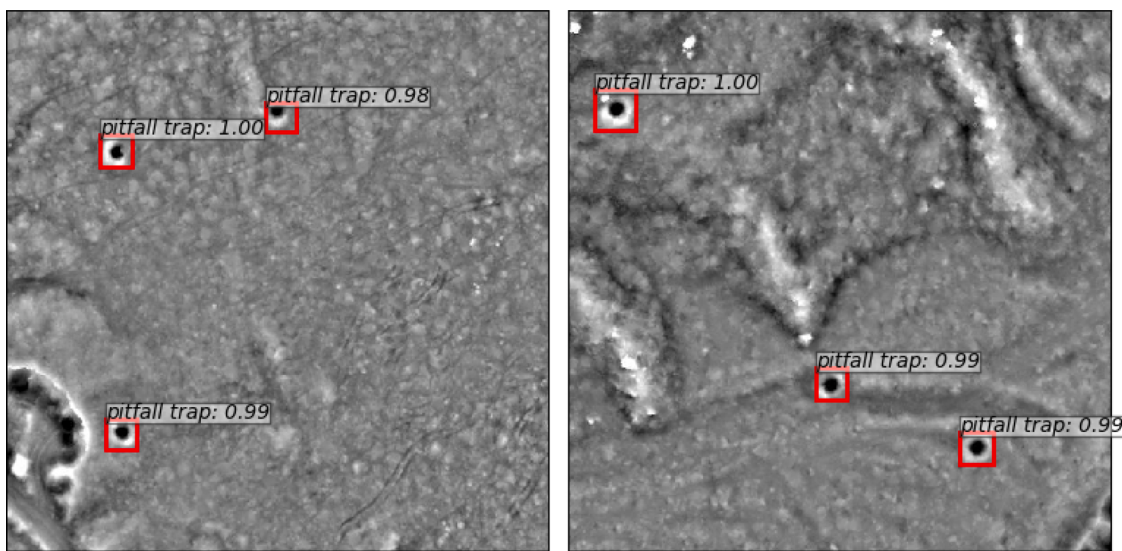
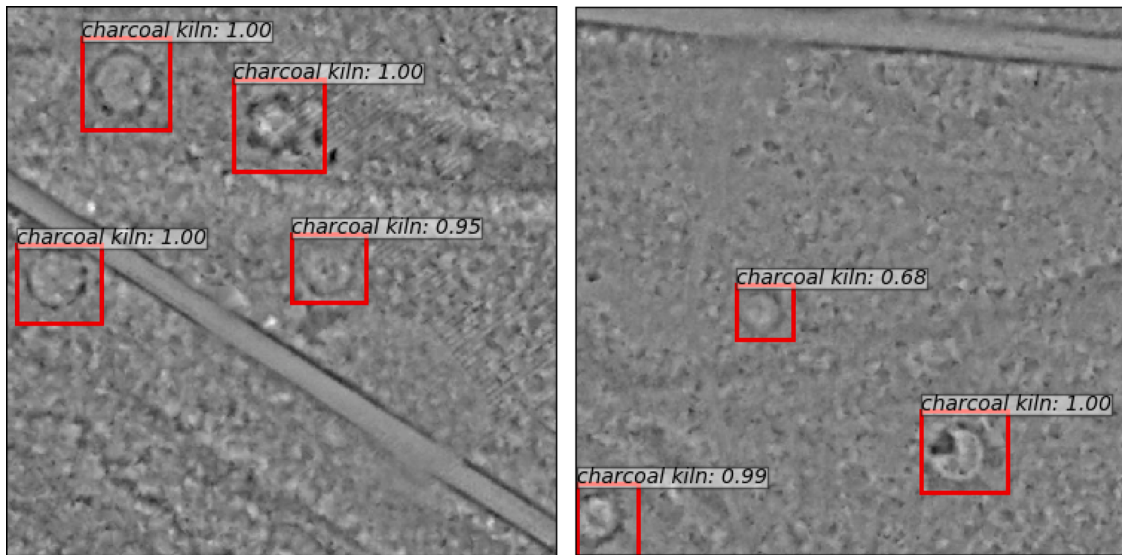


Fig. 15. Predicted grave mound locations. Each local relief model (LRM) image covers a 150 m × 150 m area.



**Fig. 16.** Predicted pitfall trap locations superimposed on LRM visualizations of ALS data.



**Fig. 17.** Predicted charcoal kiln locations superimposed on LRM visualizations of ALS data. Note that in the right hand side image, near the centre, the detected charcoal kiln had a score value of only 0.68. Usually the score value threshold was set to 0.7, in which case this true charcoal kiln would have been rejected by the automatic method.

**Table 7**

Detection results on 737 small test images of  $150\text{ m} \times 150\text{ m}$ , not seen during training, and each containing at least one cultural heritage object.

true class	predicted class				sum	count	rate
	charcoal kiln	grave mound	pitfall trap	background			
charcoal kiln	180	1	0	7	188	180	96 %
grave mound	3	603	0	109	715	603	84 %
pitfall trap	1	6	1073	161	1241	1073	86 %
background	80	252	267	0	599		
<b>consumer's accuracy</b>					2144	<b>1856</b>	87 %
wrong class					2144	11	0.5 %
false negatives					2144	277	13 %
<b>producer's accuracy</b>	68 %	70 %	80 %		2466	<b>1856</b>	75 %
false positives					2466	599	24 %
wrong class					2466	11	0.4 %

**Table 8**

Detection results on the Larvik test area.

true class	predicted class						
	charcoal kiln	grave mound	pitfall trap	back- ground	sum	count	rate
charcoal kiln	0	0	0	0	0	0	
grave mound	0	103	2	164	269	103	38 %
pitfall trap	0	0	0	0	0	0	
background	41	610	162	0	813		
<b>producer's accuracy</b>		14 %			11 %		
false positives		86 %			89 %		

**Table 9**

Results of charcoal kiln detection on Øvre Eiker municipality.

Automatic prediction	Visual inspection	Count	Percent	Count	Percent
Predicted	Confirmed	578	51 %	697	62 %
Predicted	Possible	119	11 %		
Predicted	Doubtful	135	12 %	433	38 %
Predicted	Rejected	298	26 %		
Sum predicted charcoal kilns		1130		1130	
Predicted	Confirmed	578	90 %		
Missed	Confirmed	66	10 %		
Sum confirmed charcoal kilns		644			

locations need to be checked by field visits.

The application of automated cultural heritage object detection on large amounts of ALS data immediately creates a need for visual verification of the detection results. There are some recent projects that involve citizen volunteers to help identify which automatically detected structures are true archaeological remains. In the Veluwe area in the centre of the Netherlands (Lambers et al., 2019; <https://www.zooniverse.org/projects/evakap/heritage-quest>), an internet portal is used. Participants are asked to mark every potential barrow, charcoal kiln and Celtic field within a 300 m × 300 m subimage. Each individual image is checked by at least eight different users. However, Casana (2020) argues that experts are needed for proper interpretation, and discourages the use of volunteers.

Our method is based on transfer learning, but in a setting that may not be optimal. We used a deep neural network that is pre-trained on natural scene images, followed by training on lidar visualisations with labelled cultural heritage remains. As the two types of image are quite different, there is a potential for improvement by pre-training the deep neural network on a large image set that is more similar to the lidar visualisations that we used. Gallwey et al. (2019) uses Lunar lidar data for pretraining. The obvious advantage is that the Lunar lidar data contains a large amount of craters, which are quite similar in shape to the mining pits that Gallwey et al. (2019) want to map. On the other hand, the general Lunar landscape topography may be very different from the landscapes of interest on Earth. In any event, the main purpose of pretraining is to obtain object detection capability in the deep neural network, i.e., grouping of pixels to objects parts, and grouping of object parts to objects.

In order to avoid transfer learning between unrelated image sets, several researchers are suggesting approaches to address the shortage of labelled training data. Dzeroski and Kokalj (2019) of Slovenia are starting a project in 2020 on deep clustering, where unsupervised learning of visual features is performed on remote sensing images. Two application areas are included: (1) archaeology and (2) land cover classification. Küçükdemirci and Sarris (2020) uses pre-training of a

U-net on synthetic images, for segmentation of archaeological structures in geophysical images. The synthetic images are created by inserting typical objects of interest, e.g., circles and straight lines, into images of 'background' terrain.

Even if sufficiently large sets of labelled training data were available, another issue still remains. Many of the deep neural network architectures seem to be designed with the assumption that there are usually several objects to detect in any image. However, in cultural heritage object detection and mapping, in the majority of landscapes, the absence of cultural heritage objects is much more frequent than the presence. A possible workaround suggested by Trier et al. (2019) is to add confusion classes. This was tried on the Larvik training and validation areas. False positives of all three classes were inserted into the ground truth data as 'natural mound', 'natural pit' and 'natural platform'. Then, training of the deep neural network was performed on this extended image set. Unfortunately, the detection performance did not improve. The true positive rates were slightly reduced while the false positive rates remained high. A better solution may be to look for alternative deep neural network architectures. Kramer et al. (2019) observes that the RetinaNet (Lin et al., 2020) addresses the imbalance of foreground versus background. Given the rapid development in deep neural networks in recent years, we may also expect to see further improvements in this direction in the near future.

In contrast to the major problem of high false positive rates, a minor issue, related to true cultural heritage objects being missed by the automatic method, was observed. At terrain discontinuities, e.g., a cliff, the local relief model visualisation might hide archaeological objects that were close to the terrain discontinuity. A possible solution could be to use another ALS visualisation, e.g. openness (Doneus, 2013).

In conclusion, we have demonstrated that faster R-CNN is well suited for semi-automatic detection of cultural heritage objects such as charcoal kilns, grave mounds and pitfall traps in high resolution airborne lidar data. However, it is desirable to reduce the false positive rate in order to limit the amount of visual inspection needed when the method is applied on large areas for detailed archaeological mapping.

#### CRediT authorship contribution statement

**Øivind Due Trier:** Writing - original draft, Writing - review & editing, Methodology, Software, Investigation, Validation. **Jarle Hamar Reksten:** Methodology, Software. **Kristian Løseth:** Funding acquisition, Data curation, Investigation, Validation.

#### Declaration of Competing Interest

The authors declare that they have no known competing financial interests or personal relationships that could have appeared to influence the work reported in this paper.

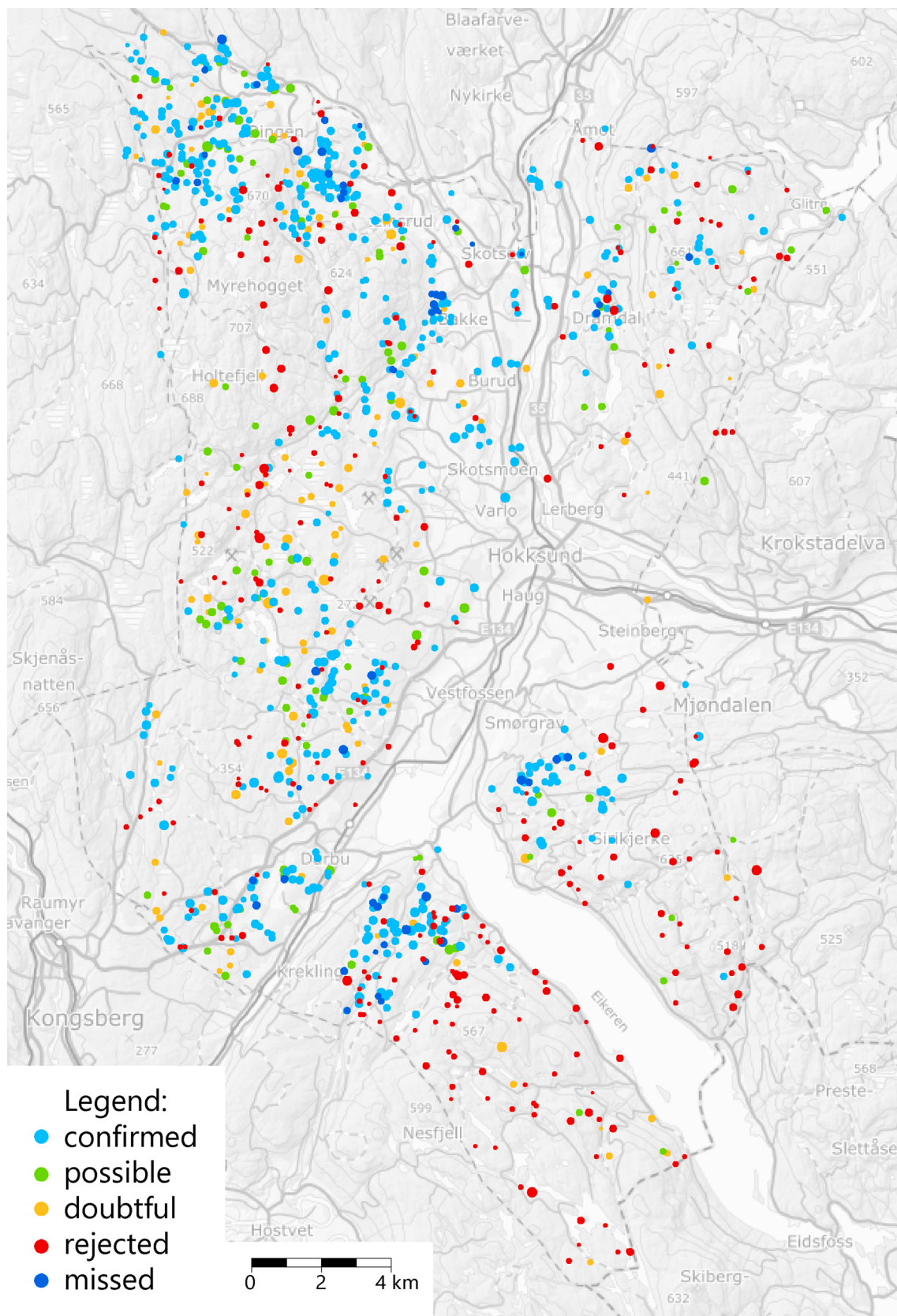


**Fig. 18.** Predicted charcoal kiln locations in Øvre Eiker municipality, Viken County.<sup>1</sup> Missed' means missed by automatic method but manually detected and confirmed. Topographic map (in grey) from <https://hoydedata.no>, the Norwegian Mapping Authority (Kartverket).

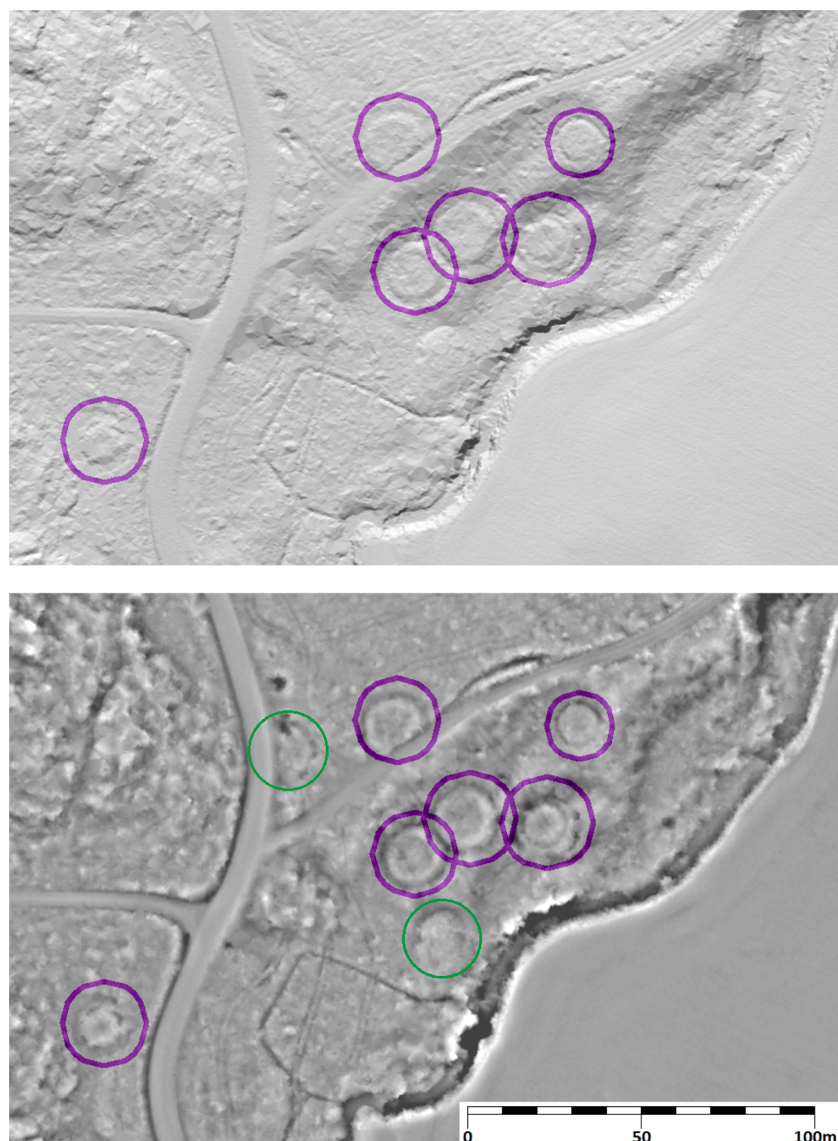


**Fig. 19.** Visual inspection of six predicted charcoal kilns (purple circles) in Øvre Eiker municipality. Top: hillshade visualization of DTM. Bottom: Local relief visualization of DTM; the green circles indicate two possible charcoal kilns that were not detected by the automatic method. The area shown is 240 m × 160 m (For interpretation of the references to colour in this figure legend, the reader is referred to the web version of this article).

## Acknowledgements

This research was funded by the Directorate for Cultural Heritage in Norway.

## Appendix A. Supplementary data

Supplementary material related to this article can be found, in the online version, at doi:<https://doi.org/10.1016/j.jag.2020.102241>.

## References

- Casana, J., 2020. Global-scale archaeological prospection using Corona satellite imagery: automated, crowd-sourced, and expert-led approaches. *J. Field Archaeol.* 45 (S1), S89–S100. <https://doi.org/10.1080/00934690.2020.1713285>.
- Doneus, M., 2013. Openness as visualization technique for interpretative mapping of airborne lidar derived digital terrain models. *Remote Sens.* 5 (12), 6427–6442. <https://doi.org/10.3390/rs5126427>.
- Dzheroski, S., Kokalj, Z., 2019. Machine learning, remote sensing and archaeology: tasks, tools, resources and needs. In: Presented at: Artificial Intelligence, Machine Learning and Deep Learning in Archaeology. 7–8 November 2019, Rome, Italy.
- Gallwey, J., Eyre, M., Tonkins, M., Coggan, J., 2019. Bringing Lunar lidar back down to Earth: mapping our industrial heritage through deep transfer learning. *Remote Sens.* 11, 1994. <https://doi.org/10.3390/rs11171994>.
- Girshick, R., Donahue, J., Darrell, T., Malik, J., 2014. Rich feature hierarchies for accurate object detection and semantic segmentation. In: IEEE Conference on Computer Vision and Pattern Recognition (CVPR). Columbus, Ohio, USA, 23–28 June 2014, pp. 580–587. <https://doi.org/10.1109/CVPR.2014.81>.
- He, K., Gkioxari, G., Dollar, P., Girshick, R., 2017. Mask R-CNN. In: The IEEE International Conference on Computer Vision (ICCV). Venice, Italy, 22–29 Oct. 2017, pp. 2961–2969. <https://doi.org/10.1109/ICCV.2017.322>.
- Hesse, R., 2010. Lidar-derived local relief models – a new tool for archaeological prospection. *Archaeol. Prospect.* 17, 67–72. <https://doi.org/10.1002/arp.374>.
- Jordhøy, P., 2008. Ancient wild reindeer pitfall trapping systems as indicators for former migration patterns and habitat use in the Dovre region, southern Norway. *Rangifer* 28 (1), 79–87. <https://doi.org/10.7557/2.28.1.152>.
- Kramer, I., Hare, J., Cowley, D., 2019. Arran a benchmark dataset for automated detection of archaeological sites on LiDAR data. In: Presented at: Artificial Intelligence, Machine Learning and Deep Learning in Archaeology. 7–8 November 2019, Rome, Italy.
- Küçükdemirci, M., Sarris, A., 2020. Deep learning based automated analysis of archaeological geophysical images. *Archaeol. Prospect.* 27 (2), 107–118. <https://doi.org/10.1002/arp.1763>.
- Lambers, K., Verschoof-van der Vaart, W.B., Bourgeois, Q.P.J., 2019. Integrating remote sensing, machine learning and citizen science in Dutch archaeological prospection. *Remote Sensing* 11, 794. DOI: 10/3390/rs11070794.

- Lin, T.-Y., Goyal, P., Girshick, R., He, K., Dollár, P., 2020. Focal loss for dense object detection. *IEEE Trans. Pattern Anal. Mach. Intell.* 42 (2), 318–327. <https://doi.org/10.1109/TPAMI.2018.2858826>.
- Ren, S., He, K., Girshick, R., Sun, J., 2017. Faster R-CNN: towards real-time object detection with region proposal networks. *IEEE Trans. Pattern Anal. Mach. Intell.* 39 (6), 1137–1149. <https://doi.org/10.1109/TPAMI.2016.2577031>.
- Ronneberger, O., Fischer, P., Brox, T., 2015. U-net: convolutional networks for biomedical image segmentation. In: Navab, N., Hornegger, J., Wells, W., Frangi, A. (Eds.), *Medical Image Computing and Computer-Assisted Intervention – MICCAI 2015*. *MICCAI 2015. Lecture Notes in Computer Science*, vol 9351. Springer, Cham, pp. 234–241. [https://doi.org/10.1007/978-3-319-24574-4\\_28](https://doi.org/10.1007/978-3-319-24574-4_28).
- Russakovsky, O., Deng, J., Su, H., Krause, J., Satheesh, S., Ma, S., Huang, Z., Karpathy, A., Khosla, A., Bernstein, M., Berg, A.C., Fei-Fei, L., 2015. ImageNet large scale visual recognition challenge. *Int. J. Comput. Vis.* 115, 211–252. <https://doi.org/10.1007/s11263-015-0816-y>.
- Simonyan, K., Zisserman, A., 2015. Very deep convolutional networks for large-scale image recognition. In: Bengio, Y., LeCun, Y. (Eds.), *Proceedings of the 3rd International Conference on Learning Representations, ICLR 2015*. San Diego, CA, USA, 7–9 May 2015. Available at: <https://arxiv.org/abs/1409.1556>.
- Solberg, B., 2015. From paganism to Christianity in Norway – an examination of graves and grave fields. In: Baug, I., Larsen, J., Mygland, S.S. (Eds.), *Nordic Middle Ages – Artefacts, Landscapes and Society. Essays in Honour of Ingvild Øye on her 70th Birthday*. University of Bergen Archaeological Series 8, pp. 275–288. Available at: <https://bora.uib.no/handle/1956/15399>.
- Trier, Ø.D., Pilø, L.H., 2012. Automatic detection of pit structures in airborne laser scanning data. *Archaeol. Prospect.* 19 (2), 103–121. <https://doi.org/10.1002/arp.1421>.
- Trier, Ø.D., Pilø, L.H., 2015. Archaeological mapping of large forested areas, using semi-automatic detection and visual interpretation of high-resolution lidar data. In: Giligny, F., Djindjian, F., Costa, L., Moscati, P., Roberts, S. (Eds.), *Proceedings of the 42nd Annual Conference on Computer Applications and Quantitative Methods in Archaeology CAA 2014–21st Century Archaeology*. Paris, France, 22–25 April 2014. Oxford: Archaeopress, pp. 81–86. Available at: <http://archaeopress.com/ArchaeopressShop/Public/displayProductDetail.asp?id={30A17C9B-F191-4734-9FD8-74C3F7002F88}>.
- Trier, Ø.D., Pilø, L.H., Johansen, H.M., 2015a. Semi-automatic mapping of cultural heritage from airborne laser scanning data. *Semata* 27, 159–186. Available at: <http://www.usc.es/revistas/index.php/semeta/article/view/2736>.
- Trier, Ø.D., Zortea, M., Tonning, C., 2015b. Automatic detection of mound structures in airborne laser scanning data. *J. Archaeol. Sci. Rep.* 2 (1), 69–79. <https://doi.org/10.1016/j.jasrep.2015.01.005>.
- Trier, Ø.D., Salberg, A.-B., Pilø, L.H., 2018. Semi-automatic mapping of charcoal kilns from airborne laser scanning data using deep learning. In: Matsumoto, M., Uleberg, E. (Eds.), *CAA2016: Oceans of Data. Proceedings of the 44th Conference on Computer Applications and Quantitative Methods in Archaeology*. Oslo, Norway, 30 March–3 April 2016. Oxford: Archaeopress, pp. 219–231. Available at: <http://archaeopress.com/ArchaeopressShop/Public/download.asp?id=%7b6A565CFE-F617-4333-9818-4C13E78B7C1B%7d>.
- Trier, Ø.D., Cowley, D.C., Waldeland, A.U., 2019. Using deep neural networks on airborne laser scanning data: results from a case study of semi-automatic mapping of archaeological topography on Arran, Scotland. *Archaeol. Prospect.* 26 (2), 165–175. <https://doi.org/10.1002/arp.1731>.
- Verschoof-van der Vaart, W.B., Lambers, K., 2019. Learning to look at LiDAR: the use of R-CNN in the automated detection of archaeological objects in LiDAR data from the Netherlands. *J. Comput. Appl. Archaeol.* 2 (1), 31–40. <https://doi.org/10.5334/jcaa.32>.